Binding of rapamycin analogs to calcium channels and FKBP52 contributes to their neuroprotective activities

Benfang Ruan*†, Kevin Pong‡, Flora Jow‡, Mark Bowlby‡, Robert A. Crozier‡, Danni Liu‡, Shi Liang‡, Yi Chen‡, Mary Lynn Mercado‡, Xidong Feng*, Frann Bennett†, David von Schack§, Leonard McDonald*, Margaret M. Zaleska‡, Andrew Wood‡, Peter H. Reinhart‡, Ronald L. Magolda*, Jerauld Skotnicki*, Menelas N. Pangalos‡, Frank E. Koehn*, Guy T. Carter*, Magid Abou-Gharbia*, and Edmund I. Graziani*¶

*Chemical and Screening Sciences, Wyeth Research, 401 North Middletown Road, Pearl River, NY 10965; ‡Discovery Neuroscience, Wyeth Research, CN8000, Princeton, NJ 08543-8000; †Discovery Inflammation, Wyeth Research, 200 Cambridge Park Drive, Cambridge, MA 02140; and §Biological Technologies, Wyeth Research, 87 Cambridge Park Drive, Cambridge, MA 02140

Communicated by Kyriacos C. Nicolaou, The Scripps Research Institute, La Jolla, CA, November 8, 2007 (received for review August 15, 2007)

Rapamycin is an immunosuppressive immunophilin ligand reported as having neurotrophic activity. We show that modification of rapamycin at the mammalian target of rapamycin (mTOR) binding region yields immunophilin ligands, WYE-592 and ILS-920, with potent neurotrophic activities in cortical neuronal cultures, efficacy in a rodent model for ischemic stroke, and significantly reduced immunosuppressive activity. Surprisingly, both compounds showed higher binding selectivity for FKBP52 versus FKBP12, in contrast to previously reported immunophilin ligands. Affinity purification revealed two key binding proteins, the immunophilin FKBP52 and the β1-subunit of L-type voltage-dependent Ca^{2+} channels (CACNB1). Electrophysiological analysis indicated that both compounds can inhibit L-type Ca^{2+} channels in rat hippocampal neurons and F-11 dorsal root ganglia (DRG)/neuroblastoma cells. We propose that these immunophilin ligands can protect neurons from Ca^{2+}-induced cell death by modulating Ca^{2+} channels and promote neurite outgrowth via FKBP52 binding.

immunophilin | L-type voltage-gated calcium channel | natural products | neurodegeneration | stroke

Immunophilin ligands, such as FK506, cyclosporin A, rapamycin, 3-normeridamycin, V-10,367, and GPI-1046, have been shown to have neuroprotective activities (1–4). Immunophilins comprise the family of FK506-binding proteins (FKBPs) having peptidyl-prolyl *cis-trans* isomerase (PPIase) activities and were proposed as likely targets for mediating this neurotrophic activity, although there is disagreement as to their specific mechanism (5–7). Over two dozen immunophilins occur in the human genome and are known to associate with a diverse array of proteins, including ion channels (7–11), steroid receptor complexes (5), transcription factors (12), and Bcl-2 upon conditional activation (6). Immunophilin ligands generate various downstream biological activities by disruption of the natural FKBP-containing complexes (5–12) or by formation of novel ternary complexes, such as FKBP12–FK506–calcineurin (13, 14) or FKBP12–rapamycin–mammalian target of rapamycin (mTOR) (15). The ternary complexes of FK506 and rapamycin with their respective protein targets result in immunosuppressive activity that may be undesirable in the context of a therapy for neurodegenerative conditions (9). FK506 and rapamycin bind multiple immunophilin isoforms, increasing the risk that off-target activities will lead to unanticipated or adverse effects. For example, the interaction of FK506 (which binds to many FKBPs) with FKBP12.6 is potentially problematic because the compound can disrupt the interaction between FKBP12.6 and the ryanodine receptor, causing Ca^{2+} leakage from endoplasmic and sarcoplasmic reticula and further resulting in impairment of the excitation–contraction coupling in cardiac muscle (9). Therefore, activities that stem from inhibition of multiple FKBPs make FK506 a problematic candidate for treating neurodegenerative conditions, even though the compound has shown efficacy in rodent models of stroke (16).

We used a structure-based drug design approach to determine whether semisynthetic analogs of rapamycin (rapalogs) that were nonimmunosuppressive and showed some selectivity for immunophilin binding might be desirable candidates for additional *in vivo* study. Reported here are the chemical syntheses of two neuroprotective, nonimmunosuppressive rapalogs, WYE-592 and ILS-920, which bind selectively to the immunophilin FKBP52 and to the β1-subunit of L-type voltage-gated calcium channels (VGCC). An investigation of the mechanistic basis of their action revealed unique interaction partners resulting in the modulation of intracellular Ca^{2+} homeostasis.

Results

Chemical Syntheses of Rapamycin Analogs. Rapamycin is a hybrid polyketide/nonribosomal peptide macrolide that forms a ternary complex of FKBP12–rapamycin–mTOR that inhibits mTOR kinase activity and leads to immunosuppression (14). To disrupt the interaction with mTOR while leaving the FKBP-binding portion of the compound intact, with the aim of reducing mTOR-mediated immunosuppressive activity while maintaining neuroprotective activity, we prepared WYE-592 from rapamycin via a [4 + 2] cycloaddition reaction with nitrosobenzene at the C1, C3 diene, and ILS-920 from further catalytic hydrogenation of WYE-592 (Fig. 1*A*). Both compounds were purified by HPLC and fully characterized (including stereochemistry) by 2D NMR analyses [supporting information (SI) Table 2].

ILS-920 is a Nonimmunosuppressive Rapamycin Analog. Inhibition of IL-2-stimulated human $CD4^+$ T cell proliferation was used as an *in vitro* measure of immunosuppression. ILS-920 showed no inhibition up to 5 μM, in contrast to rapamycin and FK506 (IC_{50} = 5 nM and 1 nM, respectively; Table 1). WYE-592 exhibited intermediate activity (IC_{50} = 150 nM) arising from a 3% conversion of the sample to rapamycin via a retro Diels–Alder reaction (data not shown), which indicated that modification at the mTOR binding

Author contributions: B.R. and K.P. contributed equally to the work. B.R., K.P., M.B., M.M.Z., P.H.R., R.L.M., J.S., M.N.P., F.E.K., G.T.C., M.A.-G., and E.I.G. designed research; B.R., K.P., F.J., R.A.C., D.L., S.L., Y.C., M.L.M., X.F., F.B., L.M., and E.I.G. performed research; B.R., K.P., M.B., R.A.C., M.L.M., D.v.S., L.M., M.M.Z., A.W., R.L.M., M.N.P., and E.I.G. analyzed data; and B.R., M.N.P., and E.I.G. wrote the paper.

Conflict of interest statement: All authors are or were employees of Wyeth and currently hold stock options in Wyeth.

¶To whom correspondence should be addressed. E-mail: graziaei@wyeth.com.

This article contains supporting information online at www.pnas.org/cgi/content/full/0710424105/DC1.

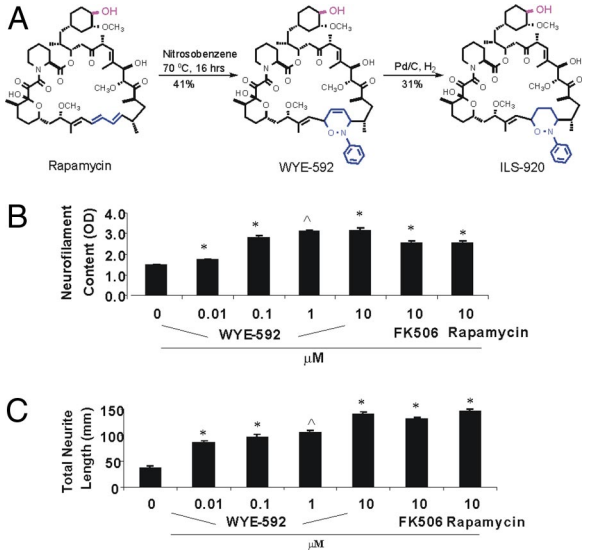

Fig. 1. Synthesis and biological activities of rapamycin analogs. (*A*) Chemical synthesis of WYE-592 and ILS-920 from rapamycin. The 42-OH (red) was derivatized and linked to the Affi-Gel 10 resin. (*B*) Effect of WYE-592 on neuronal survival. Survival of E16 rat primary cortical neurons, after treatment with control or compound for 72 h, was measured by neurofilament ELISA (*, $P < 0.01$; ^, $P < 0.001$; $n = 4$). (*C*) Effect of WYE-592 on neurite outgrowth in cortical neurons. Mean total neurite length of primary E16 rat cortical neuron cultures, after treatment with control or compound for 72 h, was measured by Cellomics ArrayScan.

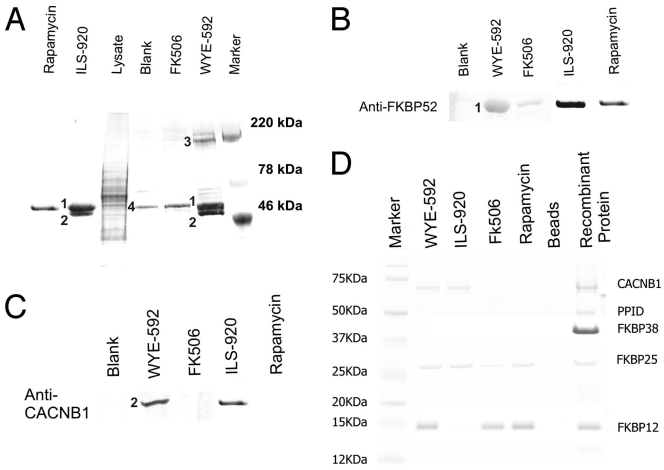

Fig. 2. Target proteins of WYE-592 and ILS-920. (*A*) Affinity precipitation of target proteins from F11 cell lysates using WYE-592, ILS-920, FK506, or rapamycin-linked affinity matrices. The bands found in the WYE-592 pull-down fraction are myosin (*3*), FKBP52 (*1*), CACNB1, FKBP25, and FKBP12 (*2*); the bands from the ILS-920 pull-down fraction are FKBP52 (*1*) and CACNB1 (*2*); and the band in the blank bead control is actin (*4*). Marker, molecular weight markers. (*B*) Western blot analysis of the affinity-precipitated proteins for the presence of FKBP52. (*C*) Western analysis of the affinity-precipitated proteins for the presence of CACNB1. (*D*) Binding of WYE-592 and ILS-920 to individual purified recombinant proteins. Each WYE-592, ILS-920, FK506, or rapamycin linked affinity matrix was incubated with purified recombinant CACNB1, PPID, FKBP38/Ca^{2+}/CaM, FKBP25, and FKBP12 separately, and individual pull-down experiments were analyzed by SDS/PAGE to assess binding affinity.

region effectively reduced the immunosuppressive activity of rapamycin by more than three orders of magnitude.

ILS-920 and WYE-592 Promote Neuronal Survival and Stimulate Neurite Outgrowth. ILS-920 and WYE-592 were found to promote neuronal survival, as measured by neurofilament ELISA in cultured rat cortical neurons (Fig. 1*B* and Table 1), with up to an order of magnitude improvement in activity versus rapamycin. The compounds also promote neurite outgrowth in both cortical neurons (Fig. 1*C*) and F-11 cells [a hybrid of rat DRG neurons and mouse neuroblastoma (17), SI Fig. 6*C*], with comparable EC_{50} values (see Table 1). Both compounds demonstrated significantly greater potency in these neuronal assays than the previously reported neuroprotective immunophilin ligand GPI-1046 (Table 1).

ILS-920 and WYE-592 Bind to FKBP52 and the β-Subunit of L-Type VGCC. With the aim of identifying putative target proteins, affinity matrices with covalently attached compound were prepared and used to precipitate proteins from F-11 cell lysates. As shown in Fig. 2*A*, three strong bands (220 kDa, 60 kDa, and 50 kDa) and two weak bands (25 kDa and 12 kDa) were found in both WYE-592 and ILS-920 pull-down fractions. Fourier-transform ion cyclotron resonance (FT-ICR) MS spectra of each band were used for Mascot searches in the National Center for Biotechnology Information (NCBI) database (SI Table 3). FKBP52 (5) and the β-subunits of the L-type VGCC (18, 19) were identified as targets of WYE-592 and ILS-920 with high *P* values, and their presence was confirmed by Western blot analysis (Fig. 2 *B* and C). FKBP25 and FKBP12 also were identified as weaker bands, whereas myosin and actin were found in all fractions, indicating nonspecific binding to the resin.

ILS-920 and WYE-592 Exhibit Highly Selective Binding to FKBP52. The observation that FKBP52 was the predominant immunophilin that was affinity-purified from F11 cell lysates with resin-bound WYE-592 and ILS-920 suggested that either FKBP52 is enriched in F11 cells relative to other immunophilins or that WYE-592 and ILS-920 exhibit binding selectivity for FKBP52. RT-PCR was carried out to measure the mRNA level of *fkbp1a* (the gene encoding FKBP12) and *fkbp4* (the gene encoding FKBP52) in F11 cells. The mRNA level of *fkbp1a* was four times higher than that of *fkbp4*, indicating that WYE-592 and ILS-920 may bind selectivity to FKBP52. To determine the specific affinity of WYE-592 and ILS-920 to FKBP52, we measured binding constants. ILS-920 and WYE-592 both demonstrated a preference for binding to FKBP52 relative to FKBP12 (229- and 8-fold, respectively) whereas FK506 and rapamycin bind to both proteins with comparable affinities (Table 1). GPI-1046 showed very weak binding affinity to both FKBP12 and FKBP52. To further probe the specificity of immunophilin/

Table 1. Biological activities and kinetic constants of immunophilin ligands

Compounds	T cell inhibition IC_{50}, μM	Neurite outgrowth EC_{50}, μM	Cortical neuron survival EC_{50}, μM	FKBP12 binding K_d, nM	FKBP52 binding K_d, nM
FK506	0.001	0.45	0.01	0.33 ± 0.03 (Lit. 0.4)	0.72 ± 0.07
ILS-920	>5	0.54	0.15	110 ± 11	0.48 ± 0.04
WYE-592	0.15	0.42	0.7	4.7 ± 0.4	0.55 ± 0.05
Rapamycin	0.005	1.6	1.3	0.33 ± 0.03	1.4 ± 0.1
GPI-1046	>5	200	8.8	>110	>12

cyclophilin interaction, and because of their reported role in neuroprotection from ischemic injury (6, 7, 12), the binding of WYE-592 and ILS-920 to purified recombinant FKBP25, FKBP38, and cyclophilin D (*ppif*) was measured [all proteins were demonstrated to be catalytically active in a peptidyl prolyl *cis-trans* isomerase assay (SI Fig. 7*A*)]. Binding of ILS-920, WYE-592, rapamycin, and FK506 to individual proteins was confirmed by affinity precipitation followed by SDS/PAGE analysis (Fig. 2*D*) or via measurement of binding constants (Table 1). To further confirm this result, the binding of [^{14}C]WYE-592 to individual proteins was measured (SI Fig. 7*B*). At 10 μM, the affinity of [^{14}C]WYE-592 binding to these targets can be ranked in the relative order: (FKBP52, FKBP12, FKBP25) $\gg$ PPID $\gg$ PPIF and FKBP38/Ca^{2+}/CaM. These results indicate that WYE-592 and ILS-920, although retaining some affinity for FKBP12 and FKBP25, have a pronounced binding selectivity for FKBP52.

ILS-920 and WYE-592 Bind to the β-Subunit of L-Type VGCC. The presence of the other key binding protein, the β1-subunit of L-type voltage-dependent Ca^{2+} channels (CACNB1), was validated by testing the binding of recombinant β1-subunit (CACNB1:*TGG548TAA*) by affinity precipitation followed by SDS/PAGE analysis; WYE-592 and ILS-920 bind to the β1-subunit but not rapamycin or FK506 (Fig. 2*C*). The binding of WYE-592 to the β1-subunit was further tested in a radioactivity assay and by protein tryptophan fluorescent quenching analysis. At 10 μM, [^{14}C]WYE-592 bound to a mutant His_6-CACNB1:*TGG548TAA* and weakly to CACNB4 (SI Fig. 7*C*). This also was confirmed by protein tryptophan fluorescent quenching (SI Fig. 7*D*), a linear dose–response indicating conformational changes upon binding WYE-592 to CACNB1. To determine whether FKBP52 and CACNB1 can associate with each other, the lysates of F11 cells in the presence or absence of 5 μM WYE-592 were immunoprecipitated with anti-FKBP52 antibody, followed by Western analysis of the immunoprecipitated fractions with anti-CACNB1 antibody to detect the coprecipitation of the β1-subunit. As shown in SI Fig. 7*E*, the β1-subunit was not coimmunoprecipitated with FKBP52 in the absence of WYE-592, indicating that FKBP52 does not associate with CACNB1 in F11 cells.

RNAi Knockdown of FKBP52 Enhanced Neurite Outgrowth. To further understand the role of FKBP52 and the β-subunit of the VGCC in mediating the neuroregenerative effects of WYE-592 and ILS-920, mRNA knockdown using siRNA was performed in cortical neurons. As shown in Fig. 3*A*, siRNA against FKBP52 and CACNB1 reduced the expression of the corresponding protein by 70–86%, whereas the expression of actin remained the same. Total neurite outgrowth was significantly increased in FKBP52 siRNA-treated neurons (125 $\pm$ 12% of control; Fig. 3 *B* and *C*) and negligibly in CACNB1 siRNA-treated neurons, which suggests that inhibition of FKBP52 stimulates neurite outgrowth, providing a strong mechanistic rationale for the neurite outgrowth observed after ILS-920 and WYE-592 treatment.

ILS-920 and WYE-592 Inhibit L-Type Ca^{2+} Current in Hippocampal Neurons and F-11 Cells. The L-type VGCC (18, 19) contains multiple subunits: a membrane-spanning α-subunit forms the Ca^{2+} channel pore, and one of four β-subunits associate with the α-subunit to regulate the gating of the channel. The β1b-, β3-, and β4-subunits are known to enhance the L-type Ca^{2+} channel current, whereas the β2-subunit plays a negative role (18, 19). Because we have shown that ILS-920 or WYE-592 bind to at least one of the β-subunits, we chose to investigate further the effect of both compounds on the function of L-type VGCC by electrophysiological analysis.

After external application of WYE-592 or FK506 to the bath solution, whole-cell Ca^{2+} currents in F-11 cells were recorded. A 49% decrease of the Ca^{2+} current density (6.5 $\pm$ 0.5 to 3.2 $\pm$ 0.3 pA/pF) was observed after incubation of WYE-592 (data not shown), similar to that observed for FK506, as has been reported (20). The effect of WYE-592 on L-type VGCC also was studied in F-11 cells by intracellular application of WYE-592. As shown in Fig. 4 *A* and *B*, upon break-in WYE-592 began to inhibit the Ca^{2+} current in F11 cells and a steady state was reached after total Ca^{2+} current was reduced by 46 $\pm$ 1.8% within 10 min. Interestingly, once a steady state was obtained with WYE-592 little further block of Ca^{2+} current was observed with the L-type VGCC antagonist BAY-K5552 (Fig. 4*B*), indicating the response to WYE-592 was predominantly on L-type VGCC current in F-11 cells. Rapamycin is reported to have no effect on L-type VGCC current (21), suggesting that WYE-592 has obtained a unique activity, relative to the parent compound, by inhibiting L-type VGCC current.

To further determine whether the observed effects on Ca^{2+} currents were specific to the modifications we had made, ILS-920 and rapamycin were tested in a more physiologically relevant context of cultured rat hippocampal neurons (Fig. 4 *C* and *D*). L-type VGCC was isolated by blockade of N-type Ca^{2+} channels with ωCTX-GVIA (100 nM). Intracellular application of ILS-920 (10 μM) resulted in inhibition of 74.5 $\pm$ 8.8% of the Ca^{2+} current after 10 min (Fig. 4 *C* and *D*, red filled circles). This response could be prevented by BAY-K5552, indicating that the inhibition was predominantly of L-type VGCC (Fig. 4*D*, red open circles). Essentially no current changes were observed in the vehicle control recordings in the presence of ωCTX-GVIA or ωCTX-GVIA plus BAY-K5552 (Fig. 4*D*, black, filled or open squares, respectively). Finally, intracellular application of rapamycin yielded no change in L-type VGCC currents (Fig. 4*D*, black filled triangles). Because ILS-920 inhibited Ca^{2+} currents in the presence of N-type blockers, but not in the presence of both L-type and N-type blockers, we conclude that ILS-920 selectively inhibits the L-type VGCC. Moreover, this effect is specific to ILS-920, because under the same conditions, rapamycin showed essentially no inhibition of the L-type VGCC.

ILS-920 Is Efficacious in a Rodent Model of Stroke. ILS-920 was selected for *in vivo* study because of its lack of immunosuppression, superior potency in *in vitro* models of neuroprotection and neuroregeneration, and pharmacokinetic profile when compared with

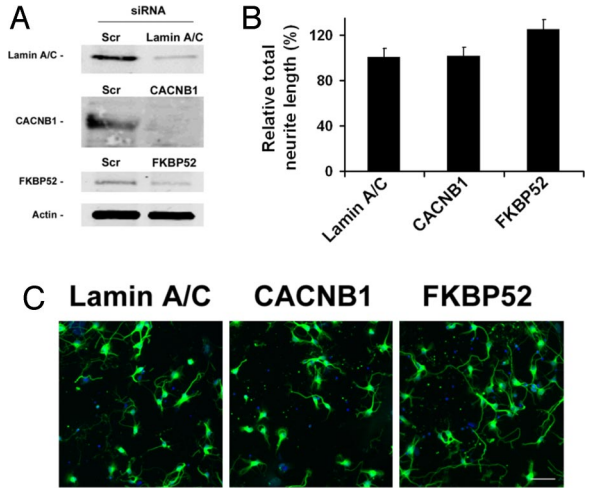

Fig. 3. Reduction of FKBP52 and β1-subunit of VGCC by siRNA and the effect on neurite outgrowth. (*A*) Expression of the corresponding proteins in cortical neurons with and without siRNA treatment. (*B*) Total neurite outgrowth in cortical neurons in response to siRNA knockdown of CACNB1 ($P = 0.39$) and FKBP52 ($P = 0.039$) normalized to lamin A/C (control) knockdown. (*C*) Representative images of cortical neurons treated with siRNA against lamin A/C, CACNB1, or FKBP52 after 24 h. (Scale bar: 40 μm.)

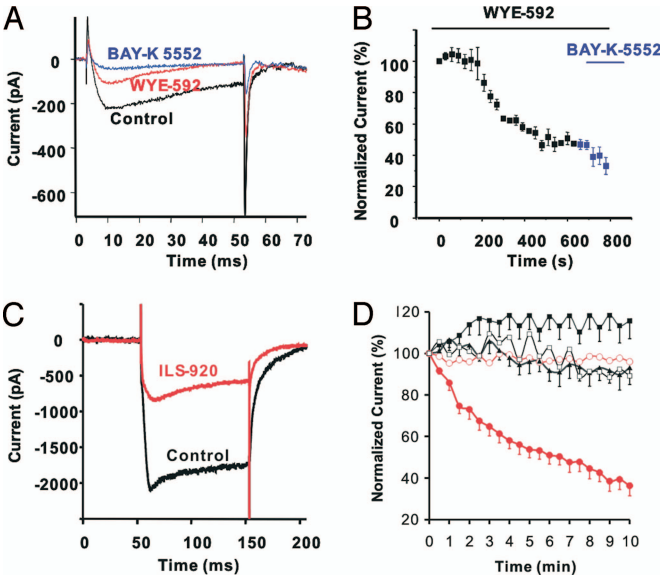

Fig. 4. WYE-592 and ILS-920 inhibition of L-type Ca^{2+} channels. (*A*) Representative Ca^{2+} current traces from F-11 cells after 10 μM WYE-592 was applied internally by the recording pipette. Currents are shown at time 0 s (black trace), at time 800 s (red trace, inhibition by WYE-592), and in the presence of the L-type Ca^{2+} channel blocker BAY-K 5552 (blue trace). (*B*) Time course (same experiment as in *A*; $n = 3$) of Ca^{2+} current reduction in F-11 cells after intracellular application of 10 μM WYE-592 at 0 s and then followed by bath application of 10 μM BAY-K5552 at 600 s. (*C*) Representative Ca^{2+} current traces after intracellular application of 10 μM ILS-920 to hippocampal neurons in the presence of bath-applied 100 nM ωCTX GVIA. Traces shown are from time 0 s (black trace) and 10 min (red trace). (*D*) Averaged time courses of whole-cell Ca^{2+} currents recorded from hippocampal neurons, normalized to the initial current (current at 0 s), and plotted as mean ± SEM. Relative Ca^{2+} current changes were recorded for 10 min after internal application of vehicle (0.1% DMSO, black filled squares, $n = 6$), rapamycin (black filled triangles, $n = 11$), and ILS-920 (red filled circles, $n = 10$) in neurons recorded in extracellular solution containing 1 μM TTX plus 100 nM ωCTX-GVIA, as well as after intracellular application of vehicle (DMSO 0.1%, black open squares, $n = 6$) and ILS-920 (red open circles, $n = 10$) in neurons recorded in external solution containing 1 μM TTX plus 100 nM ωCTX-GVIA plus 10 μM BAY-K 5552.

WYE-592. In a transient middle cerebral artery occlusion (tMCAO) model of ischemic stroke, ILS-920, administered 4 h post-occlusion at 10 and 30 mg/kg, significantly reduced infarct volume by 24% and 23% in 72 h, respectively, (Fig. 5), as well as robustly enhanced functional recovery measured by improvement in neurological deficits (data not shown). In contrast, rapamycin alone in a similar model for stroke was reported to be devoid of efficacy (16).

Discussion

After reports that the immunosuppressant drugs FK506 and rapamycin exhibit potent neuroprotective activities (1, 2), numerous attempts to develop therapeutically useful compounds by uncoupling neuroprotection from immunosuppression in this class of compounds have met with limited success. Nonimmunosuppressive immunophilin ligands such as GPI1046, which contains the FKBP-binding moiety of rapamycin and FK506 but lacks an mTOR or calcineurin binding domain, have been pursued as potential therapies for neurodegenerative disorders. GPI1046 has been reported to stimulate neurite outgrowth in chicken sensory ganglia at picomolar concentrations and to stimulate recovery after sciatic nerve crush (22). However, other reports represent the neuroprotective activity of GPI1046 as being marginal in neurite outgrowth studies in chicken DRG explants, rat DRGs, and a sciatic nerve injury model (23, 24). In view of these discrepancies, it was proposed that neuroprotection is mediated by immunophilins other than

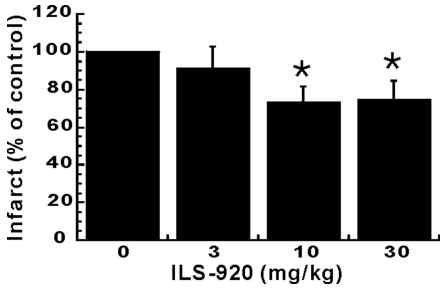

Fig. 5. *In vivo* efficacy in a stroke model. At 4 h post-tMCAO, ILS-920 was administered as an i.v. bolus at 3, 10, and 30 mg/kg, respectively. Neuroprotective efficacy was measured by reduction of ischemic infarct at 72 h after treatment with ILS-920 ($P < 0.05$).

FKBP12, notably FKBP52 and FKBP38 (5, 6). We therefore set out to design and synthesize rapamycin analogs that demonstrated substantially reduced immunosuppressive and improved neuroprotective activities with the aim of using the resultant compound to determine whether immunophilin binding alone is important for neuroprotection.

Rather than eliminating the mTOR binding domain of rapamycin to generate small molecules like GPI1046, we introduced an additional bulky group at the rapamycin triene to disrupt mTOR binding (15) and eliminate immunosuppressive activity. WYE-592 contains a bulky group at the mTOR binding region of rapamycin that was installed via a Diels–Alder reaction with nitrosobenzene. This compound was twice as potent a promoter of cortical neuronal survival than rapamycin and four times more potent at stimulating neurite outgrowth (Table 1). Surprisingly, the compound exhibited a significant (although reduced) level of immunosuppressive activity, relative to rapamycin, as measured by IL-2-stimulated T cell proliferation. A small percentage conversion of WYE-592 to rapamycin via a retro Diels–Alder reaction, however, can account for this level of activity, and indeed 3% rapamycin was observed after 72 h incubation of WYE-592 in assay buffer (data not shown). Reduction of the C2,C3 olefin in WYE-592 via catalytic hydrogenation to yield ILS-920 precluded the possibility of such a retro Diels–Alder reaction in the product, and the compound was observed to have no effect on T cell proliferation up to 5 μM. Moreover, ILS-920 was almost five times more potent than WYE-592 at promoting cortical neuronal survival (and therefore an order of magnitude more potent than rapamycin). Both compounds demonstrated greater activity in these neuronal assays than the previously reported nonimmunosuppressive immunophilin ligand GPI-1046 (22–24).

We further sought to determine which, if any, immunophilins were binding partners for ILS-920 and WYE-592 and whether these or any other nonimmunophilin proteins might mediate the compounds' neuroprotective activities. Affinity purification from F-11 cell lysates, using resin with covalently bound WYE-592 and ILS-920, identified FKBP52 and the β1-subunit of L-type Ca^{2+} channels (CACNB1) as the major binding partners for the compounds. Moreover, ILS-920 and WYE-592 demonstrated an unanticipated and intriguing feature—binding selectivity for FKBP52 over FKBP12. We have shown that FK506 and rapamycin have only a 2- to 3-fold difference in binding affinity to FKBP12 versus FKBP52. ILS-920 demonstrated over 200-fold selectivity for FKBP52 versus FKBP12, representing a change in binding specificity (as measured by the ratio of K_d FKBP52/K_d FKBP12) of three orders of magnitude relative to rapamycin (Table 1). This binding selectivity is unexpected, because x-ray structures of the isomerase domains of FKBP12 and FKBP52 are very similar and the active site residues have only 1 aa difference (His-87 in FKBP12 versus Ser-118 in FKBP52) (25). It therefore is likely that in the process of interfering with mTOR binding, the introduction of conformation-

ally constrained substitutions at the triene of rapamycin can subtly influence the overall global population of macrolactone conformers that in turn affects immunophilin binding selectivity, given that rapamycin is well known to be a dynamic molecule that exists as a set of major and minor solution conformers because of *cis-trans* isomerization of the amide bond (12, 26). This report presents evidence that modification distant to the FKBP-binding domain of rapamycin could generate orders of magnitude changes in immunophilin binding selectivity.

Recently, FKBP52, FKBP38/Ca^{2+}/CaM, and cyclophilin D have been proposed as the specific mediators of the neuroprotective action of immunophilin ligands (5–7). However, there is disagreement as to whether a single immunophilin mediates this activity and, if so, which one. FKBP52 was proposed to mediate the neurite outgrowth action of FK506 through activation of steroid receptor complexes that mediate downstream responses to estrogen, androgen, and glucocorticoid hormones (5). An FKBP38-calmodulin-Ca^{2+} complex formed at high Ca^{2+} concentrations recently was proposed to mediate Ca^{2+}-overload-induced cell death through its interaction as a negative effector of the antiapoptotic Bcl-2 protein (6). Cyclophilin D, the *Ppif* gene product involved in mitochondrial permeability transition pore assembly, also was proposed to mediate Ca^{2+} overload and oxidative stress-induced cell death after ischemia (7). However, ILS-920 and WYE-592 showed a strong affinity for FKBP52 but no binding to FKBP38/Ca^{2+}/CaM and cyclophilin D. Together with our observation that neurite outgrowth was significantly increased in FKBP52 siRNA-treated neurons, FKBP52 appears to be a principal mediator of neurite outgrowth of WYE-592 and ILS-920, given that neurite outgrowth of this magnitude is consistent with the reported activity of anti-FKBP52 antibody (5).

ILS-920 and WYE-592 represent the first immunophilin ligands that have been shown to bind to the β1-subunit and inhibit L-type VGCC. L-type VGCC play a pivotal role in neuronal functioning, because Ca^{2+} influx through the L-type channel regulates important transcriptional responses such as the CaM kinase IV (CaMKIV)-dependent pathway, mitogen-activated protein kinase (MAPK) signaling pathway, cAMP response element binding protein (CREB)-dependent transcription, NFAT-dependent transcription, and apoptosis pathway (27–31). These pathways are known to play critical roles in synaptic plasticity, neural inflammation, developmental cell death, and neurodegenerative disorders (27–31). Because ILS-920 inhibited Ca^{2+} currents in the presence of N-type blockers, but not in the presence of both L-type and N-type blockers, we conclude that ILS-920 selectively inhibits the L-type VGCC, although we cannot exclude the possibility that other VGCC (such as P/Q or R) also may contribute to some lesser degree. Moreover, this effect is specific to ILS-920, because under the same conditions, rapamycin showed essentially no inhibition of the L-type VGCC. It therefore is likely that attenuation of Ca^{2+} influx is mechanistically important for neuroprotection, because Ca^{2+} overload generally is considered to be a critical event in excitotoxic-mediated neuronal death (28).

Having prepared nonimmunosuppressive rapalogs with improved neuroprotective properties, identified their binding partners, and established a link between these proteins and the compounds' biological activities, we further sought to evaluate their activity in an *in vivo* model of stroke. ILS-920 was selected as a suitable candidate for testing based on its lack of immunosuppression, superior potency, and pharmacokinetic properties in addition to its improved stability relative to WYE-592 (see above). Treatment with ILS-920 at 10 and 30 mg/kg, administered 4 h postocclusion, significantly reduced infarct volume and improved neurological recovery in a tMCAO model of ischemic stroke. The *in vivo* efficacy of ILS-920 is in marked contrast to rapamycin, which failed to reduce infarct volume in a rat tMCAO model (16). GPI-1046 also was reported to have limited or no efficacy in comparable models of ischemic stroke (24). *N*-(*N*′,*N*′-dimethylcarboxamidomethyl)cycloheximide (DM-CHX) was reported to reduce infarct volume by up to 44% when delivered via intracerebroventricular (i.c.v.) application 2 h postocclusion (but not 6 h) in a rat model of endothelin-induced transient focal ischemia (6). Because i.c.v. application is impractical for human stroke patients, in the absence of data employing alternate routes of delivery it is unclear at present what the clinical utility of such a compound might be. FK506 also has been reported to protect against ischemic insult (16), although its immunosuppressive activity and other off-target activities (9) also limit the therapeutic utility of the compound. In contrast, treatment with ILS-920 results in significant enhancement of neurological recovery in a tMCAO model of stroke with at least a 4-h therapeutic window (time elapsed between insult and initial dose) when delivered intravenously. Interestingly, modulation of calcium transients are implicated in both the proposed FKBP38 and cyclophilin D-mediated pathways of neuroprotection, as well as for the calcineurin/calmodulin pathway inhibited by FK506. The additional capacity of ILS-920 to promote neurite outgrowth, mediated by binding to FKBP52, may serve to further extend the therapeutic window of the compound beyond the acute phase of recovery from ischemic injury. Together, our results indicate that perhaps both FKBP52 and Ca^{2+}-channel-mediated signaling pathways are required for clinically relevant *in vivo* efficacy in stroke models.

In conclusion, our work presents evidence that modification of rapamycin at the mTOR binding region can provide nonimmunosuppressive compounds with unanticipated selectivity for FKBP52, inhibition of L-type Ca^{2+} channel currents, and significant efficacy in an animal model of ischemic stroke. The *in vivo* efficacy of ILS-920 derives from the compound's dual functions as an potential activator of glucocorticoid and other steroid receptors via dissociation of FKBP52 from the receptor complexes and as an inhibitor of L-type VGCC via binding to the β1-subunit.

Materials and Methods

Protocols for well established procedures (affinity matrix syntheses, kinetic analysis of immunophilin ligands, cloning and expressing recombinant genes and binding assays, preparation of neuronal cultures, transient MCAO, and immunosuppression assays) can be found in the *SI Methods*.

Materials. Chemicals were purchased from Sigma-Aldrich (St. Louis, MO). Antibodies were from Abcam (Cambridge, MA). Media, human ORF clones (*cacnb1*, *cacnb4*, *fkbp3*, *fkbp4*, *fkbp8*, *ppiF*, and *ppiD*), plasmids (pDEST17), and SuperScript system were from Invitrogen (Carlsbad, CA). Protein purification kits were from Pierce (Rockford, IL) or Qiagen (Valencia, CA). TOPTip P-4 column was from Glygen (Columbia, MD). Ni-chelated flash plates and [^{3}H]FK506 were from PerkinElmer Life Science (Boston, MA). PCR reagents and Affi-Gel 10 were from BioRad (Hercules, CA).

Synthesis of WYE-592. Rapamycin (0.3 g, 0.328 mmol) was dissolved in 5 ml of toluene with gentle heating. To this solution was added, dropwise, a solution of nitrosobenzene (0.1 g, 3 equivalents) in 5 ml of toluene. The reaction mixture was stirred at 70°C for 16 h, and then the products were chromatographed via reversed-phase HPLC (column: 250 × 20 mm YMC ODS-A with 50 × 20 guard; mobile phase: 80 to 85% methanol:water in 40 min, flow = 20 ml/min) to yield 0.139 g of WYE-592 (42% yield, >99% purity; SI Table 2). [^{14}C]WYE-592 (5 mCi, specific activity 241 mCi/mmol) was prepared by a similar method.

Synthesis of ILS-920. WYE-592 (0.29 g, 0.284 mmol) was dissolved in 7 ml of methanol in an 18-mm test tube, and a spatula tip of Pd/C catalyst (Aldrich) was added. The mixture was hydrogenated on a Parr apparatus for 15 min at 2.0 atmosphere H_2. The products were chromatographed via reversed-phase HPLC (column: 250 × 20 mm YMC ODS-A with 50 × 20 guard, mobile phase: 80% methanol:water for 15 min, then to 85% in 5 min, then held at 85% for 20 min, flow = 20 ml/min) to yield 0.089 g of ILS-920 (31% yield, >99% purity; SI Table 2)

Affinity Precipitation of Drug Targets and Western Analyses. F11 cells were grown in culture medium, DMEM supplemented with 10% FBS, and 1% penicillin/streptomycin in 75-cm^2 vented flasks in a 37°C incubator with 5% CO_2. Cells were harvested at 80% confluence and washed with PBS buffer. To 3 × 10^8 cells, 2 ml of lysis buffer (50 mM Tris, pH 7.4, 250 mM NaCl, 5 mM EDTA, 50 mM NaF, 1 mM Na_3VO_4, 1% Nonidet P-40, 0.1% mercaptoethanol, and 2% protease

inhibitor cocktails) was added, and its S-100 supernatant was collected after a 15-min centrifugation at 4°C. Aliquots (2 ml) were incubated with affinity matrices (100–150 μl) at 4°C. After washing with lysis buffer (2 ml) and then PBS buffer (2 ml), beads were analyzed by SDS/PAGE. The protein bands were cut and digested with trypsin (0.3 μg) in digestion buffer (30 μl; 0.2% NH_4HCO_3) at 30°C. The resulting peptides (2 μl) were loaded into a nanoelectrospray tip of a Bruker (Billerica, MA) APEXII FT-ICR mass spectrometer equipped with an actively shielded 9.4 T superconducting magnet (Magnex Scientific Ltd., U.K.), and an external Bruker Apollo ESI source, and mixed with 1% formic acid in methanol (2 μl). A voltage of ≈ -800 V was applied between the nanoelectrospray tip and the glass capillary. The mass spectra data were externally calibrated by using HP tuning mix and used for a Mascot search in the NCBI protein databases. Reasonable protein candidates were selected based on confidence scores (*P* value). For Western analysis, the proteins obtained from the affinity matrices were separated by SDS/PAGE, transferred to PVDF membranes by electroblotting (100 V, 1 h), immunoblotted with the anti-CACNB1 or anti-FKBP4 antibody, and visualized by 3,3′,5,5′-tetramethylbenzidine (TMB) staining.

Transient Transfection of siRNA into Primary Cortical Neurons. For each condition, 5×10^5 cortical neurons were transfected with 200 ng of scrambled siRNA (Dharmacon RNA Technologies, Boulder, CO), siGLO lamin A/C siRNA (Dharmacon), L-type calcium channel β1-subunit siRNA [5′-GGAGAAGUACAAUAAUGACTT-3′ (sense) and 5′-GUCAUUAUUGUACUUCUCCTT-3′ (antisense)] or FKBP4 siRNA [5′-CCUAGCUAUGCUUUUGGCATT-3′ (sense) and 5′-UGCCAAAGCAUAGCUAGGTT-3′ (antisense)] (Ambion, Inc., Austin, TX) by using program DC-104 on the 96-well shuttle (Amaxa Biosystems, Gaithersburg, MD). Then 25 μl from each transfection reaction were added to a poly(D)-lysine-coated 96-well plate (four wells per experiment). Transfected cortical neurons were maintained in culture for 24 h.

Western Blotting Analyses. Cortical neurons treated with scrambled siRNA, lamin A/C, CACNB1, or FKBP52 siRNA were lysed in RIPA buffer containing protease inhibitor mixture and phosphatase inhibitors, and protein concentrations were measured with a Bradford assay (Bio-Rad Laboratories, Hercules, CA). Two micrograms of protein per condition were loaded into each well and separated via SDS/PAGE. Proteins were transferred onto nitrocellulose and incubated with an antibody against lamin A/C (Upstate), CACNB1 (Abcam, Cambridge, MA), or FKBP52 (Santa Cruz Biotechnology), and actin (Sigma) as a loading control. Bands were developed and quantified by using an Odyssey Infrared Imaging System and Odyssey software (Li-Cor Biosciences, Lincoln, NE). Protein expression knockdown was calculated as the ratio to actin as a percentage of scrambled siRNA expression ($79.2 \pm 13.7\%$ for lamin A/C, $70.8 \pm 20.8\%$ for CACNB1, and 86.8 ± 7.0 for FKBP52, $n = 3$).

Whole-Cell Patch-Clamp Recordings. The whole-cell configuration of the patch-clamp technique was used to record Ca^{2+} currents from cells at room temperature by using an EPC-9 amplifier (HEKA InstruTECH Corp.) with the acquisition and analysis program Pulse-PulseFit from HEKA (Lambrecht, Germany). Electrodes were fabricated by using a P-87 puller (Sutter Instrument). Electrodes had a resistance of 2–5 MΩ when filled with recording solution (140 mM CsCl, 10 mM EGTA, 10 mM Hepes, 5 mM $MgCl_2$, 2 mM ATP, and 1 mM cAMP, pH 7.2). The standard bath recording solution is Ca^{2+}- and Mg^{2+}-free HBSS (pH 7.4) containing 10 mM Hepes, 10 mM dextrose, and 4 mM $BaCl_2$. Currents were filtered at 3 kHz, and the inward Ca^{2+} currents were recorded from cells held at -90 mV with 10 mV depolarizing steps from -80 mV to 60 mV for 50 ms for characterization, or to 0 mV for 50 ms (F-11) or 100 ms (neurons) once every 30 s for compound experiments. Saturating concentrations of N-type and L-type Ca^{2+} channel blockers were used in the indicated experiments.

ACKNOWLEDGMENTS. We thank Bob Abraham and Frank Walsh for critical discussions and Robert P. Smith, Patric Stenberg, Marshall Siegel, Girija Krishnamurthy, Sue McElhiney, Maya Singh, Ker Yu, Beatriz Carreno, Mary Collins, Mia Summers, Laurel Barbieri, Huiyu Yang, Bradley Haltli, Mike May, Ann Aulabaugh, and Christine Li for help and advice.

1. Lyons WE, George EB, Dawson TM, Steiner JP, Snyder SH (1994) Immunosuppressant FK506 promotes neurite outgrowth in cultures of PC12 cells and sensory gangli. *Proc Natl Acad Sci USA* 91:3191–3195.
2. Steiner JP, *et al*. (1997) Neurotrophic actions of nonimmunosuppressive analogues of immunosuppressive drugs FK506, rapamycin, and cyclosporin A. *Nat Med* 3:421–428.
3. Marshall VL, Grosset DG (2004) GPI-1485 Guilford. *Curr Opin Invest Drug* 5:107–112.
4. Summers MY, Leighton M, Liu D, Pong K, Graziani EI (2006) 3-Normeridamycin: A potent non-immunosuppressive immunophilin ligand is neuroprotective in dopaminergic neurons. *J Antibiot* 59:184–189.
5. Gold BG, Densmore V, Shou W, Matzuk MM, Gordon HS (1999) Immunophilin FK506-binding protein 52 (not FK506-binding protein 12) mediates the neurotrophic action of FK506. *J Pharmacol Exp Ther* 289:1202–1210.
6. Edlich F, *et al*. (2006) The specific FKBP38 inhibitor *N*-(*N*′,*N*′-dimethylcarboxamidomethyl)cycloheximide has potent neuroprotective and neurotrophic properties in brain ischemia. *J Biol Chem* 281:14961–14970.
7. Baines CP, *et al*. (2005) Loss of cyclophilin D reveals a critical role for mitochondrial permeability transition in cell death. *Nature* 434:658–662.
8. Pong K, Zaleska MM (2003) Therapeutic implications for immunophilin ligands in the treatment of neurodegenerative diseases. *Curr Drug Tar CNS Neurol Dis* 2:349–356.
9. Lam E, *et al*. (1995) A novel FK506 binding protein can mediate the immunosuppressive effects of FK506 and is associated with the cardiac ryanodine receptor. *J Biol Chem* 270:26511–26522.
10. Cameron AM, *et al*. (1995) Immunophilin FK506 binding protein associated with inositol 1,4,5-trisphosphate receptor modulates calcium flux. *Proc Natl Acad Sci USA* 92:1784–1788.
11. Sinkins WG, Goel M, Estacion M, Schilling WP (2004) Association of immunophilins with mammalian TRPC channels. *J Biol Chem* 279:34521–34529.
12. Galat A, Lane WS, Standaert RF, Schreiber SL (1992) A rapamycin-selective 25-kDa immunophilin. *Biochemistry* 31:2427–2434.
13. Kissinger CR, *et al*. (1995) Crystal structures of human calcineurin and the human FKBP12–FK506-calcineurin complex. *Nature* 378:641–644.
14. Liu J, *et al*. (1991) Calcineurin is a common target of cyclophilin-cyclosporin A, FKBP-FK506 complexes. *Cell* 66:807–815.
15. Choi J, Chen J, Schreiber SL, Clardy J (1996) Structure of the FKBP12–rapamycin complex interacting with the binding domain of human FRAP. *Science* 273:239–242.
16. Sharkey J, Butcher SP (1994) Immunophilins mediate the neuroprotective effects of FK506 in focal cerebral ischaemia. *Nature* 371:336–339.
17. Platika D, Boulos MH, Baizer L, Fishman MC (1985) Neuronal traits of clonal cell lines derived by fusion of dorsal root ganglia neurons with neuroblastoma cells. *Proc Natl Acad Sci USA* 82:3499–3503.
18. Opatowsky Y, Chen CC, Campbell KP, Hirsch JA (2004) Structural analysis of the voltage-dependent calcium channel β subunit functional core and its complex with the α1 interaction domain. *Neuron* 42:387–399.
19. Pichler M, *et al*. (1997) β subunit heterogeneity in neuronal L-type Ca^{2+} channels. *J Biol Chem* 272:13877–13882.
20. Yasutsune T, *et al*. (1999) Vasorelaxation and inhibition of the voltage-operated Ca^{2+} channels by FK506 in the porcine coronary artery. *Br J Pharmacol* 126:717–729.
21. Norris CM, Blalock EM, Chen KC, Porter NM, Landfield PW (2002) Calcineurin enhances L-type Ca^{2+} channel activity in hippocampal neurons: Increased effect with age in culture. *Neuroscience* 110:213–225.
22. Steiner JP, *et al*. (1997) Neurotrophic immunophilin ligands stimulate structural and functional recovery in neurodegenerative animal models. *Proc Natl Acad Sci USA* 94:2019–2024.
23. Harper S, *et al*. (1999) Analysis of the neurotrophic effects of GPI-1046 on neuron survival and regeneration in culture and *in vivo*. *Neuroscience* 88:257–267.
24. Bocquet A, *et al*. (2001) Failure of GPI compounds to display neurotrophic activity *in vitro* and *in vivo*. *Eur J Pharmacol* 415:173–180.
25. Wu B, *et al*. (2004) 3D structure of human FK506-binding protein 52: Implications for the assembly of the glucocorticoid receptor/Hsp90/immunophilin heterocomplex. *Proc Natl Acad Sci USA* 101:8348–8353.
26. Kessler H, Haessner R, Schüler W (1993) Structure of rapamycin: An NMR, molecular-dynamics investigation. *Helv Chim Acta* 76:117–130.
27. Bito H, Deisseroth K, Tsien RW (1996) CREB phosphorylation and dephosphorylation: A Ca^{2+}- and stimulus duration-dependent switch for hippocampal gene expression. *Cell* 87:1203–1214.
28. Ghosh A, Greenberg ME (1995) Calcium signaling in neurons: Molecular mechanisms and cellular consequences. *Science* 268:239–247.
29. Impey S, *et al*. (1998) Cross talk between ERK, PKA is required for Ca^{2+} stimulation of CREB-dependent transcription and ERK nuclear translocation. *Neuron* 21:869–883.
30. Graef IA, *et al*. (1999) L-type calcium channels and GSK-3 regulate the activity of NF-ATc4 in hippocampal neurons. *Nature* 401:703–708.
31. Augustine GJ, Santamaria F, Tanaka K (2003) Local calcium signaling in neurons. *Neuron* 40:331–346.